A Further Development of the Chromaticity Technique for Satellite Mapping of Suspended Sediment Load

Tommy Lindell and *Bert Karlsson*
National Environmental Protection Board, Environmental Quality Laboratory, 750 08 Uppsala, Sweden
Mats Rosengren
Swedish Space Corporation, 171 54 Solna, Sweden
Tom Alföldi
Applications Technology Division, Canada Centre for Remote Sensing, Ottawa, Ontario K1A 0Y7, Canada

ABSTRACT: A further development of the technique for mapping suspended sediment load using the chromaticity method is presented. The calibration is based on several Landsat scenes from Sweden and Canada covering different atmospheric conditions and different solar angles. The method is continuously used for water quality surveillance of Swedish lakes.

INTRODUCTION

THE CHROMATICITY TECHNIQUE, as described originally by Munday and Alföldi (1975), has been used for water quality mapping in Sweden for several years. Munday and Alföldi's approach has been further developed, and this paper describes an advanced system for automatic mapping of suspended sediment load using a microcomputerized system. The chromaticity system as modified uses absolute radiance values from the satellite and explicitly treats solar angle variations and atmospheric disturbances. Comparisons with an extensive amount of field data have been made.

The purpose of our study was to develop a method suited for operational water quality surveillance from Landsat, and to find a technique that eliminated or at least limited the amount of field data necessary for calibration. Another important goal was an economical system. To make the method economically feasible, a microcomputer was used for evaluation. However, this limits the use of time-consuming algorithms.

HARDWARE FACILITIES

A Swedish made image processing system called EBBA was used, based on a microcomputer system Metric-85 (similar in size to the "Apple") supplied with an image memory, a color display, a tape recorder, and a color printout. The Metric-85 has a 62K memory and two floppy disc drives each with a storage capacity of 150 K. The EBBA image memory has three image planes with a capacity of 256 by 256 pixels (times eight bits deep) each and there are also four graphical planes of 256 by 256 (times one bit), one of which is always white. The other three graphical planes could be colored in any combination of red, green, and blue in intensities of 0 to 255. The Sony Trinitron color display presents 256 by 256 images in any combination of red, green, and blue.

CHARACTERISTICS OF LANDSAT DATA

The digital data used for processing were usually obtained from the Esrange Landsat Station (ELS), Kiruna, Sweden and the EROS Data Cent (EDC), Sioux Falls, South Dakota. Computer compatible tapes (CCTs) acquired from EDC were system corrected in the old X-format produced before 1979, and the ELS CCTs were specially corrected with only radiometric corrections applied. No resampled data were used for the original calibration. The radiometric correction algorithms used by the stations are different, resulting in different radiometric calibrations on CCT's acquired from different sources. The algorithms used at ELS for radiometric calibration and correction of MSS data are based on calibration wedge data transmitted from the satellite together with MSS image data combined with relative sensor to sensor correction to minimize striping. The method used is identical to the so-called CAL 3 calibration method developed and used by the Canada Centre for Remote Sensing (CCRS) described by Ahern and Murphy (1978). Nominal minimum and maximum radiances, corresponding to digital values 0 to 255 on CCTs, are given for Landsats 1 to 3 in Table 1. The values given for Landsats 2 and 3 in the table are the same for CCRS and ELS.

PHOTOGRAMMETRIC ENGINEERING AND REMOTE SENSING,
Vol. 52, No. 9, September 1986, pp. 1521–1529.

0099-1112/86/5209-1521$02.25/0

TABLE 1. NOMINAL MAXIMUM AND MINIMUM RADIANCES.

		EROS (CAL 2) (mW/cm²sr)			
		4	5	6	7
Landsat 1	R_{max}	2.48	2.00	1.76	Not calibrated
	R_{min}	0.0	0.0	0.0	0.0
Landsat 2	R_{max}	2.63	1.76	1.52	3.91
	R_{min}	0.08	0.06	0.06	0.11
Landsat 3	R_{max}	2.50	2.00	1.65	4.50
	R_{min}	0.04	0.03	0.03	0.03
		CCRS/ELS (CAL 3) (mW/cm²sr)			
		4	5	6	7
Landsat 1	R_{max}	3.00	2.00	1.75	Not calibrated
	R_{min}	0.0	0.0	0.0	0.0
Landsat 2	R_{max}	3.00	2.00	1.75	4.00
	R_{min}	0.0	0.0	0.0	0.0
Landsat 3	R_{max}	2.50	2.00	1.75	4.00
	R_{min}	0.0	0.0	0.0	0.0

THE METHOD USED FOR MAPPING OF SUSPENDED SEDIMENT LOAD

The most commonly used method of assessing water quality from Landsat data is based on correlation between water quality variables and linear combinations of Landsat MSS-bands. However, this requires an extensive reliance on ground truth information, which must be available for each Landsat scene or even subscene. Therefore, it is important to find a tool better suited to operational use which will compensate for solar angle effects and atmospheric disturbances.

The chromaticity mapping method as described by Munday and Alföldi (1975) and later developed in several papers, e.g., Alföldi and Munday (1978) and Munday and Alföldi (1979), provides some advantages in mapping by normalizing for total radiance. This eliminates disturbances affecting all bands in the same proportion such as purely geometric solar angle effects.

The chromaticity indices x and y are calculated as a ratio of Landsat MSS radiances where

$$x = B_4/(B_4+B_5+B_6), \quad (1)$$

$$y = B_5/(B_4+B_5+B_6), \quad (2)$$

B_i = the *radiances* of the Landsat bands

i = 4,5,6.

The x and y describe the color of the object as seen by the Landsat MSS when the brightness or total radiance is removed. Because the calculation is based on Landsat MSS radiances, it is necessary to use radiometrically calibrated Landsat data (not always available from all Landsat receiving stations worldwide).

The chromaticity transformation has been shown to be promising when attempting to eliminate atmospheric disturbances using only the image data itself. The atmospheric adjustment possibilities were further discussed by Munday (1983).

In order to make necessary calibrations, lake water samples were taken in the field at the same time as the satellite passage. Typically, samples have been taken within a few hours of the passage time and, at the most, one day apart. However, sample sites were chosen mostly in isolated lake basins to limit rapid water quality changes in the respective basins. Analysis of suspended load has been performed according to standard methods (Strickland and Parsons, 1972) and is comparable with Munday *et al.* (1980). In addition, sampling was performed for temperature, turbidity, secchi disk depth, and sometimes for chlorophyll *a*. (Lindell, 1980, 1981; Lindell and Rosengren, 1981; Lindell *et al.*, 1985). Analyses other than suspended load were used for different types of comparisons and corrections.

EXTRACTION OF IMAGE INFORMATION FOR THE CALIBRATION

For comparisons between field data and image data, extraction of information was performed on the EBBA-system using a standard software package. The procedure calculates mean, standard deviation, pixel number and a histogram of the frequency distribution.

To be able to enhance the radiometric resolution and to sample the image in a statistically and "physically" acceptable manner, we need at least 25 pixels and, due to residual striping from the six detectors of each MSS band, at least a coverage of six scan lines of information. The most practical might be to define a sample box of 6 by 6 pixels. In general, when reducing the geometric resolution by averaging over an area of n pixels, the radiometric resolution or the signal-to-noise ratio is increased by a factor $\sqrt{n}$. In the case of a 6 by 6 box, the radiometric resolution is increased by a factor of six times. Due to the fact that some lakes are small and some areas narrow, the sampling box has in some cases been rather irregular and elongated.

Data from the field and the image were then compared after taking into account the calculations for absolute radiance, solar angle, and atmospheric adjustment. The details of these procedures are discussed below.

SOLAR ANGLE NORMALIZATION

The spectral distribution of the solar radiation changes considerably as the airmass is penetrated. The *balance* of solar irradiation reaching the ground within different Landsat MSS spectral bands changes with solar angle, as illustrated by Figure 1. For a wide range of solar angles the chromaticity of an object measured by Landsat MSS is strongly affected. Solar angle effects were discussed by Munday and Alföldi (1979) and were found not to affect the chromaticity analysis to any disturbing degree. However, in that paper a rather limited range of sun elevation angles (33 to 52 degrees) was used when performing the study and, therefore, the effect probably was negligible. The MSS data for Sweden have covered a much larger range of sun elevation angles (14 to 52 degrees) and, thus, the

effect is more pronounced, especially at lower sun elevations.

We have chosen to separate the treatment of sun elevation effects on the illumination of the objects from other effects of variation in atmospheric conditions.

The solar angle normalization is generalized using a fixed atmospheric model. Basic data concerning the spectral distribution of solar radiation for different optical air-masses have been taken from Kondratyev (1969), and the spectral responses of the different Landsat MSS spectral bands were obtained from Markham and Barker (1982). Calculations leading to Table 2 and Figure 1 are based on these data. Optical airmass as a function of solar angle is found in Kondratyev (1969) or approximated by

$$m = 1/\sin(h), \tag{3}$$

where m is the optical air mass and h is the sun elevation angle.

The solar irradiance at the ground within a spectral band varies according to

$$I_{m,i} = I_{o,i}\,\tau_i^m \tag{4}$$

where $I_{m,i}$ = solar irradiance on ground at optical airmass m within spectral band i,
$I_{o,i}$ = extraterrestrial solar irradiance in spectral band i, and
τ_i = atmospheric transmission constant for spectral band i,

$I_{o,i}$ and τ_i calculated for Landsat 1–3 MSS bands 4 to 7 are found in Table 2 and the same data calculated for Landsats 4 and 5 MSS bands 1 to 4 are found in Table 3.

If we want to perform a solar angle correction using a sun elevation of 90° (zenith) as reference corresponding to an optical airmass $m = 1$, the solar angle corrected radiance in Landsat band i can be calculated according to

$$B_{i,s} = B_i\,\tau^{1-m}{}_i \tag{5}$$

where $B_{i,s}$ = calculated solar angle corrected or normalized radiance in spectral band i, and
B_i = measured Landsat MSS radiance.

As $B_{i,s}$ values are used only to calculate chromaticity, only factors affecting the *balance* between MSS bands are accounted for, leaving out simple geometric effects.

TABLE 2. LANDSAT 1–3 MSS SOLAR ANGLE NORMALIZATION CONSTANTS.

	Band			
	4	5	6	7
$I_{o,i}$ (relative units)	54.1	45.2	39.0	62.5
τ_i	0.882	0.935	0.969	0.986

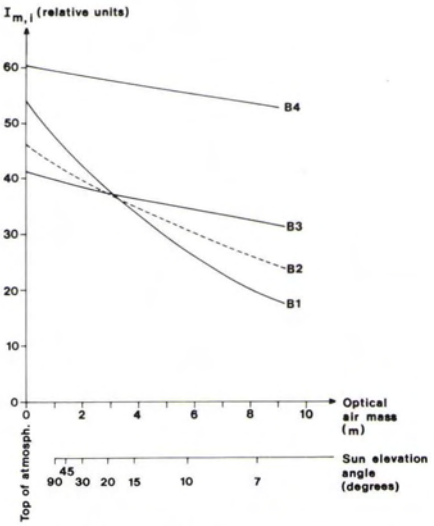

FIG. 1. Relative solar irradiance on the ground at different sun elevation angles within Landsat 4 and 5 MSS spectral bands (calculated from Kondratyev (1969) and Markham and Barker (1982)).

TABLE 3. LANDSAT 4–5 MSS SOLAR ANGLE NORMALIZATION CONSTANTS.

	Band			
	1	2	3	4
$I_{o,i}$ (relative units)	53.7	45.8	41.0	60.2
τ_i	0.885	0.932	0.970	0.986

The procedure (if normalizing to 90°) used here results in rather high correction factors, and, thus, in the future a correction to a lower solar angle might be considered to minimize nonlinear effects not taken care of by the atmospheric adjustment procedures used.

ATMOSPHERIC ADJUSTMENT PROCEDURE

The working hypothesis of the chromaticity approach (see Munday and Alföldi, 1975) is that, if corrections of the Landsat band radiances are made for solar elevation angle, atmospheric conditions, *etc.*, then the chromaticity values for water in any location in any scene will lie on a curve, here called the "universal calibration curve."

The objective here is to find a good approximation of this curve. Given a certain number of Landsat scenes where the atmospheric conditions within any one scene or subscene can be considered uniform, for each scene a number of locations are given with

solar angle-corrected chromaticity values x_s, y_s given by

$$x_s = B_{4,s}/(B_{4,s}+B_{5,s}+B_{6,s}) \quad (6)$$
$$y_s = B_{5,s}/(B_{4,s}+B_{5,s}+B_{6,s}) \quad (7)$$

where $B_{4,s}$, $B_{5,s}$, and $B_{6,s}$ are their solar angle corrected radiance values.

If the chromaticity approach is valid then the chromaticity values of the scenes, after atmospheric adjustments have been made to a reference atmospheric condition, should lie close to the universal calibration curve.

The influence of a change in atmospheric condition of a given scene is not known in detail, so a hypothesis has to be made. The one adopted in this paper is based on findings by Munday and Alföldi (1979) and Munday (1983). The technique is similar to the one used by CCRS, Canada. Certain changes due to the character of the data have been made and our approach will be the following:

Let L_i, $i=1,2,\ldots,I$, denote I number of loci and suppose that loci L_i has N_i number of locations. The solar angle-corrected chromaticity values for location j ($j=1,2,\ldots,N_i$) in loci L_i will be denoted $(x_s^{(i)}(j), y_s^{(i)}(j))$.

Given a linear hypothesis for the impact of an atmospheric variation on the chromaticity values of the location j, the atmospheric corrected values $(x_{as}^{(i)}(j), y_{as}^{(i)}(j))$ are related to the old ones by

$$x_{as}^{(i)}(j) = x_w + t_i(x_s^{(i)}(j) - x_w), \quad (8)$$
$$y_{as}^{(i)}(j) = y_w + t_i(y_s^{(i)}(j) - y_w), \quad (9)$$

where t_i is some (not yet known) non-negative real number, common for all locations within locus i (i.e., independent of j) and (x_w,y_w) is the white point at 90° solar angle.

Let $F = (f_b; b \in B)$ denote a family of curves f_b with graphs in the chromaticity plane and parametrized by an index set B. For example, if the family of curves is the set of all second order polynomials, then a typical f_b can be expressed by

$$f_b(x) = b_0 + b_1x + b_2x^2,\ b = (b_0,b_1,b_2) \in \mathbf{R}^3. \quad (10)$$

Let d denote the Euclidean distance function in the chromaticity plane; i.e., if (x_1,y_1) and (x_2,y_2) are two points in the plane, then

$$d^2((x_1,y_2),(x_2,y_2)) = (x_1-x_2)^2 + (y_1-y_2)^2. \quad (11)$$

The distance d_b from a point (x,y) to a graph of some function f_b in F is then naturally defined as

$$d_b((x,y),f_b) = \min_u d((x,y),(u,f_b(u))). \quad (12)$$

We may now define a measure of the distance for a set of loci to a function in F by

$$D_b^2 = \sum_{i=1}^{I}\sum_{j=1}^{N_i} d_b^2((x_{as}^{(i)}(j),y_{as}^{(i)}(j)),f_b), \quad (13)$$

when the loci are subjected to atmospheric correction expressed by the numbers t_i, $i=1,2,\ldots,I$.

The expression D_b is dependent on the still unknown parameters t_i, $i=1,2\ldots,I$ and b, defining the function f_b in F. These will be determined by minimizing the expression D_b over all non-negative t-values and all b in the index set B. To avoid the trivial solution (all $t_i = 0$ and f_b any curve passing through the white point (x_w,y_w) which gives minimum value zero), it will be assumed that at least one of the loci, say L_1, needs no atmospheric correction, i.e., $t_1=1$. In general, all knowledge available should be taken into account to decide whether a certain t_i-value should be kept equal to 1 (no haze) or to be free to vary (subject to haze).

If t_i, $i=1,2,\ldots,I$ ($t_1=1$) and b are the parameter values for which D_b^2 assumes the minimum, the conclusions that the t-values define reasonable physical atmospheric corrections of the loci and that the function f_b in F approximates the true universal calibration curve well, should of course be subjected to a close investigation before accepted. The data could of course be insufficient to determine the universal calibration curve by this method.

It should be noted that the minimization cannot in general be expressed in terms of linear regression.

From a practical point of view, it is hard to work with d_b itself; instead, we may use the definition of d and, instead of D_b, consider D defined by

$$D^2 = \sum_{i=1}^{I}\sum_{j=1}^{N_i} d^2((x_{as}^{(i)}(j),y_{as}^{(i)}(j)),(u_j^{(i)},f_b(u_j^{(i)}))), \quad (14)$$

where $u_j^{(i)}$ is some point on the curve f_b associated with the location j in loci L_i. D^2 is then dependent on the unknown parameters t_i, $i=1,2,\ldots I$, b and $u_j^{(i)}$, $j=1,2,\ldots,N_i$, $i=1,2\ldots,I$. The minimization of D^2 over these parameters (with $t_1=1$, say) will yield the same result as for D_b because

$$\min_{t,b,u} D^2 = \min_{t,b}\min_{u} D^2 = \min_{t,b} D_b^2. \quad (15)$$

The t-values obtained define the atmospheric correction for the respective loci.

If L is any other locus than the L_i's used to determine f_b, its atmospheric correction is determined by minimizing D^2 for a single locus by keeping b fixed and equal to the b above while minimizing D^2 with respect to the t-value associated with L.

For the minimization process, the subroutine ZXCGR in the IMSL (International Mathematical Statistical Library) has been employed. For the data presented here, the family of curves first considered was the family of polynomials of degree at most 2. However, the range of chromaticity values was too limited to obtain reliable values of the second order term of the polynomial, so only polynomials of first degree were used in the sequel. For data sets with locations with very high concentrations of suspended matter (not yet mapped by us in Sweden), a second-order term must certainly be taken into account.

CALIBRATION OF SUSPENDED MATTER VERSUS CHROMATICITY

It is of great interest to investigate the possibility to predict concentration of suspended matter from the chromaticity values. Several models have been proposed for this problem, e.g., a linear model of $\ln(S)$ to chromaticity (Munday and Alföldi, 1979). The data presented here give a high correlation (about 0.92) for this model (x $v.$ $\ln(S)$). If very low concentrations of suspended matter are contained in the data set, a more natural model would probably be the linear model of $\ln(S+1)$ to chromaticity.

For the data, a calculation was made to find the best linear model of transformed S-data to chromaticity using a Bayesian method (Box and Tiao, 1973, ch. 10). The transformations of S are considered where $((S+p_2)^{p_1}-1)/p_1$, for p_1 in the range $-1(0.1)1$ and p_2 in $0(1)10$. The result of the analysis gives support to the $\ln(S+1)$ model (Figure 2).

The *complete set* of calibration data is shown in Figure 3 where the suspended sediment is along the y-axis and the chromaticities are along the x-axis. After solar angle normalization and atmospheric adjustment, the result is demonstrated in Figure 4. The linear correlation coefficient after the solar angle and atmospheric corrections is as high as 0.9 with 120 data points from four different scenes.

THE MAPPING PROCEDURE

The above discussion has dealt mainly with the creation of a synthetic (generalized) suspended sediment load locus, which is of theoretical interest. For the practical mapping problems, the same type of atmospheric adjustment procedure as discussed above (Equations 8 and 9) may be applied. Another solution has been applied at CCRS (Munday and Alföldi, 1979). If, however, the discussed hypothesis

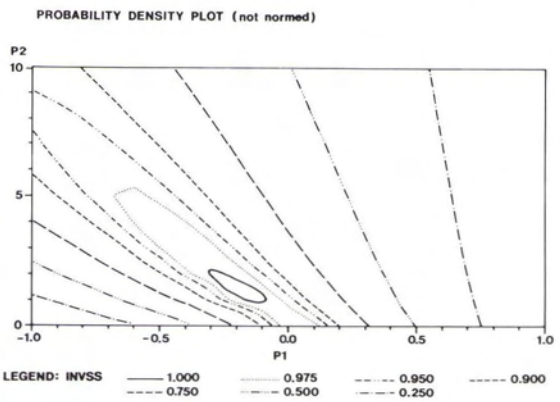

FIG. 2. Contours of the posterior distribution (unnormalized) of p_1, p_2 given the data S for the transformation $((S+p_2)^{p_1}-1)/p_1$ using a standard prior distribution of Box and Tiao. The area of highest probability density is in the neighborhood of the point (0,1) which corresponds to the $\ln(S+1)$ transform.

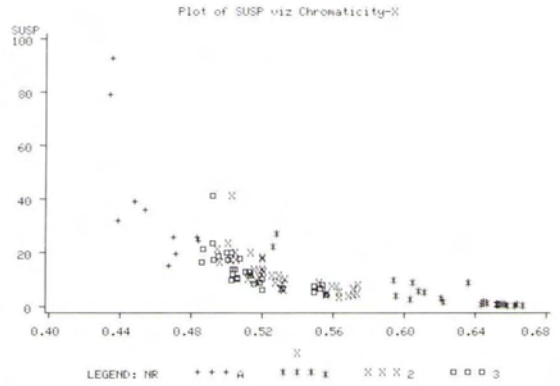

FIG. 3. Plot of suspended sediment load (mg/l) versus chromaticity x for four different data sets (scenes).

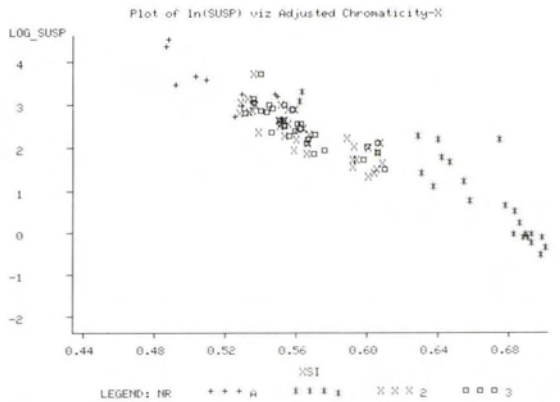

FIG. 4. Plot of ln suspended sediment load versus x after solar angle and atmospheric adjustments.

of the atmospheric influence on the chromaticity is correct, then a simpler technique may be used. Instead of referring data to a reference locus, the angular direction from the white point may be calibrated directly to suspended sediment load, as the sediment load should be equal in certain directions assuming linearity. This means, however, moving from a bulk subscene correction to pixelwise correction.

The complete mapping procedure will then contain the following steps:

- A binary mask covering land is created by interactively determining a threshold for MSS band 7.
- Landsat MSS bands 4 to 6 are smoothed outside the land mask using a 6 by 6 (or 6 by 4 to save time) pixel filter for unresampled data (due to the fact that each MSS band has six sensors).
- The chromaticity transformation (x,y) is then performed taking into account the radiometric corrections of Table 1 and solar angle normalization.
- An atmospheric adjustment is made by moving the present locus to the reference locus. Alternatively,

angular directions from the white point are directly converted to suspended sediment load figures.
- Pseudocolor scales are applied to fit the calibration. A standardized logarithmic scale is applied for suspended sediment load.
- The result is presented on the color screen and photographed for documentation. An ink jet plotter hard copy map is used as final output from the system (Plate 1).

RESULTS

Results from the mapping of suspended matter using the technique described are presented in the form of maps (Plate 1). The example shown here is from Lake Mälaren in the middle of Sweden showing the spring situation (13 May 1981) from Landsat 2 and using a geometrically precision corrected CCT.

PREDICTION POWER OF CHROMATICITY TECHNIQUE

To be able to get some understanding of the accuracy of the chromaticity approach, we have used a number of data collected in 1979. In the absence of relevant verification data of suspended load, we used transmissivity data, and a regression technique was used to generate transmissivity data for Lake Mälaren. These data were compared to independently collected field data. No systematic deviation was detected between measured and predicted values. The paired t-test of the difference resulted in a t-value of 0.14 and probability ($|t|>0.14$) = 0.88 ($n=201$) under the null-hypothesis that the expected mean of the differences is zero. The high probability value of 0.88 confirms that there is no reason to reject the null-hypothesis.

The result is very convincing (Figure 5) but it also points out the limitations of the method. The very difficult problem of interference with some types of chlorophyll is clearly shown here. The samples marked **o** were collected in an area with heavy occurrences of *Oscillatoria*. These areas should be avoided when mapping, which was pointed out in an earlier paper (Lindell, 1981). On omitting those areas, the correlation between recorded and calculated data is very high. Still, when looking at data from different basins (different symbols of the Figure) of the lake, there is a clear indication of separation, which most likely is due to different types of phytoplankton. We can foresee that, with the better radiometric resolution of Landsat TM, we might be able to map this variable still better and also be able to separate organic and inorganic matter.

DISCUSSION

One critical phase of this technique is the calculation of absolute radiances. Our experience is that the receiving stations are not always that conscientious when creating a CCT. Our experiences cover literally hundreds of CCTs from ELS, and several inadequacies have come to light since the start in 1978. Our experience with Landsat MSS digital data from several other receiving stations prompts us to warn the reader to be cautious in accepting such data at face value.

In the image producing phase we have made some modifications of the original technique as presented by Munday and Alföldi. The first modification concerns the values used to define the solar radiation and its response in the MSS. The values used here for solar radiation have been extracted from Kondratyev (1969) and those concerning the Landsat sensor characteristics are from Markham and Barker (1982). As Munday and Alföldi hypothesized that the chromaticity transformation itself removed solar angle differences, the results here are slightly different from theirs.

Our original reference data set has a clearly defined locus for suspended sediment with a well defined relationship between x and y in the chromaticity diagram. However, the relationship between x-y and the suspended matter is so far a function that should be determined cumulatively, which means that future data may slightly modify our calibration.

One of the largest advantages with the atmospheric adjustment technique used here is the fact that all data necessary are contained in the image data itself. This makes it convenient for operational use.

In a recently introduced alternative technique, the atmospheric adjustment may even be avoided by the use of calibration between suspended sediment load and angular directions from the white point.

There are, of course, possibilities to make atmospheric adjustments in several other ways, but all corrections involving physical data of the atmospheric conditions are both troublesome to use and often doubtful in representativity. Corrections of this type have been used for CZCS images (Sörensen, 1979). Some attempts have also been made for Landsat data by Forster (1984) but his approach includes 23 steps, which in our case, with a microcomputer and few field data, limits the operational use.

No comparisons between all the different approaches have been made, which is why it is too early to judge the validity of the different results achieved. MacFarlaine and Robinson (1984) discussed different atmospheric adjustment algorithms among them the chromaticity technique (p. 567), but apparently they used only digital counts and not absolute radiances. Their results are, therefore, of no significance when judging for the accuracy of the chromaticity technique.

Apart from atmospheric disturbances, other complications which might occur include bottom reflectance and, as discussed above, the chlorophyll content of the water. These components have not been studied here. Bukata (1983) criticized the chromaticity technique in this respect, but the limitations of its applicability had already been pointed

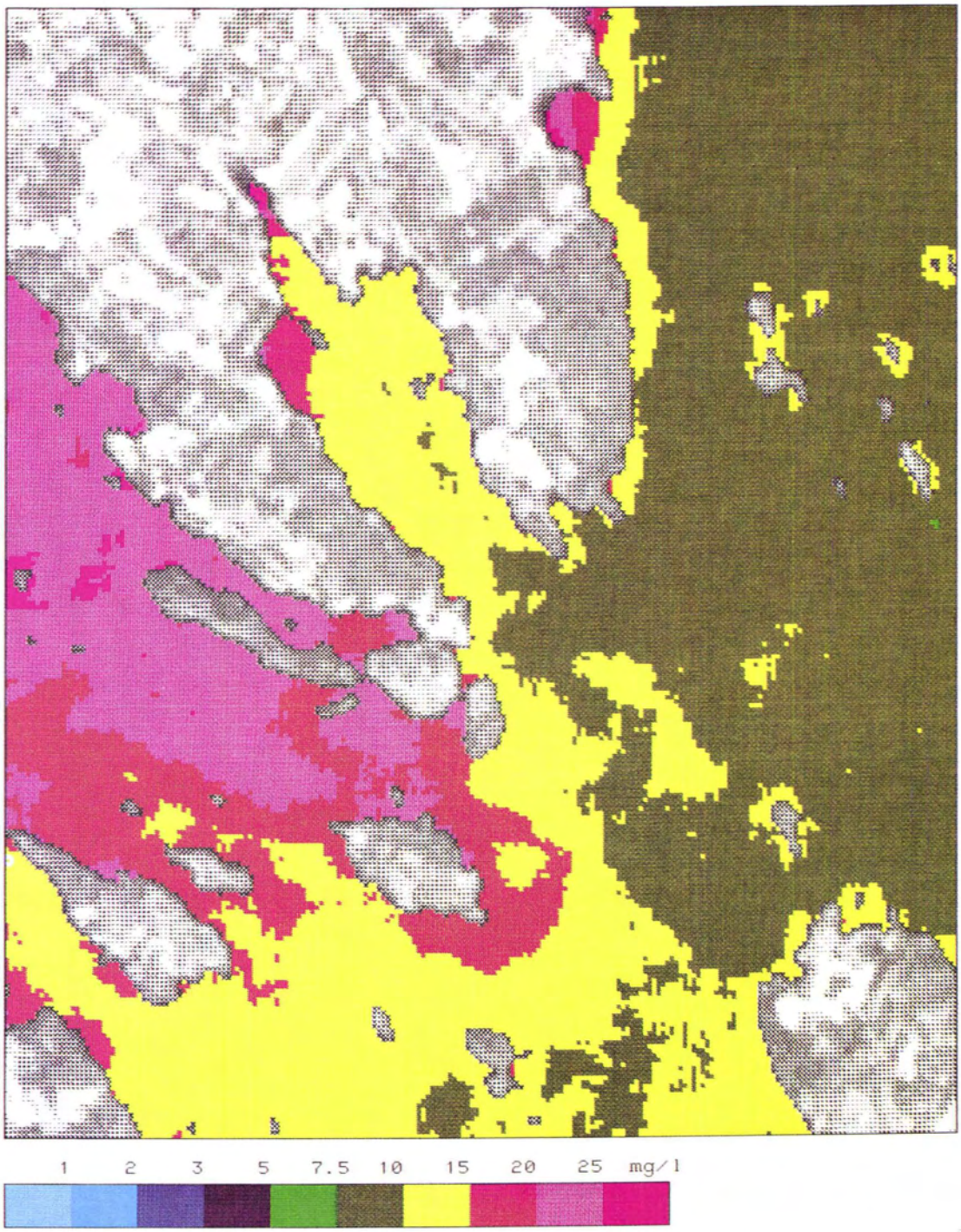

PLATE 1. Suspended sediments in Lake Mälaren, a geometrically precision corrected Landsat-2 scene of 13 May 1981.

out, and discussed in detail by Alföldi and Munday (1978).

Several authors have discussed the use of resampled data for water quality assessment, arguing about the "synthetic" pixel-values created by the resampling (e.g., Verdin, 1983). We consider this problem to be completely theoretical and of no practical interest. Besides, the resampling puts the spectral

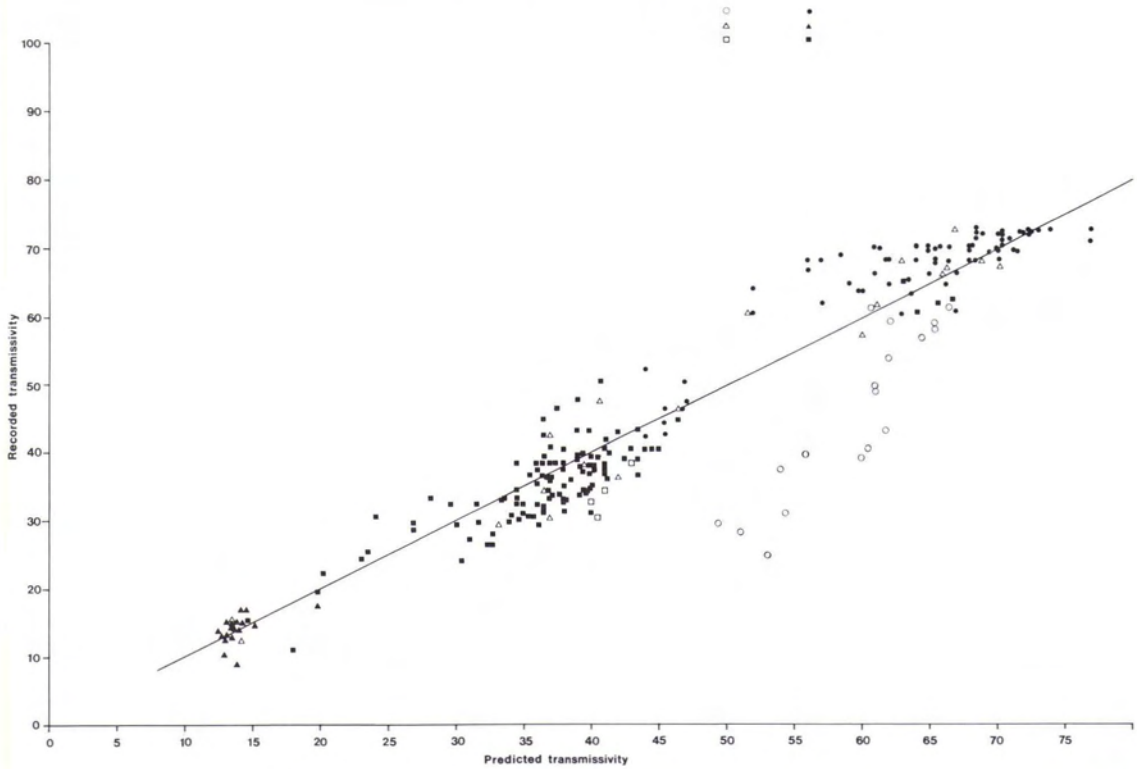

FIG. 5. Verification of transmissivity recordings, Lake Mälaren, 28 September 1979. o denotes area with *Oscillatoria redekei*.

bands on top of each other, which is a necessity in multi-spectral analysis. Pixels along the shoreline are very seldom of any water quality value as they may be mixed land/water pixels or affected by bottom reflectance or vegetation. They should, therefore, be neglected in the interpretation anyway.

CONCLUSIONS

The utility of Landsat is strongly dependent upon the quality of the Landsat data and the manner in which the data are extracted. It is possible to extract data for a certain subscene and obtain good correlation between the Landsat signal and the (sampled) lake quality. However, to apply such a procedure to the whole Landsat scene, or still worse, to try to compare results from other scenes, is rather risky with different regression techniques. The investigator must seriously contend with environmental variables such as solar angle, sediment type, and atmospheric conditions, as well as system variables related to the preprocessing of the digital data by the receiving station. For most purposes we recommend radiometrically corrected data and, for the chromaticity technique, it is mandatory.

The chromaticity technique for suspended solids analysis continues to develop through the efforts of several investigators world-wide. It represents a viable operational method which overcomes several forms of environmental noise.

REFERENCES

Ahern, F. J., and J. Murphy, 1978. *Radiometric calibration and correction of Landsat 1, 2, and 3 MSS data*. Res. Rept 78-4 CCRS, Energy, Mines and Resources Canada.

Alföldi, T., and J. C. Munday, 1978. Water quality analysis by digital chromaticity mapping of Landsat data. *Canadian Journal of Remote Sensing*, Vol. 4, No. 2, pp. 108–126.

Box, G. E. P., and G. C. Tiao, 1973. *Bayesian inference in statistical analysis*. Addison-Wesley, Reading, Mass.

Bukata, R. P., 1983. Use of chromaticity in remote measurements of water quality. *Remote Sensing of Environment*, Vol. 13, No. 2, pp. 161–177.

Forster, B. C., 1984. Derivation of atmospheric correction procedures of LANDSAT MSS with particular reference to urban data. *Int. J. Remote Sensing*, Vol. 5, No. 5, pp. 799–817.

Kondratyev, K. Y., 1969. *Radiation in the atmosphere*. Academic Press.

Lindell, L. T., 1980. *Kalibrering av Landsatdata för kartering av vatten-kvaliteten i Mälaren*. Swed. Env. Prot. Bd PM 1266.

———, 1981. Experiences from correlations of Landsat data versus transmission of light and chlorophyll a. *Verh. Internat. Verein. Limnol.* 21, pp. 438–441.

Lindell, L. T., and M. Rosengren, 1981. Country-wide mapping of the water quality of Sweden using Landsat imagery. *4ème Colloque International du G.D.T.A.*, Toulouse, p. 408.

Lindell, L. T., Steinvall, M. Jonsson, and Th. Claesson, 1985. Mapping of coastal-water turbidity using Landsat imagery. *Int. J. of Rem. Sens.* Vol. 6, No. 5, pp. 629–682.

MacFarlane, N., and I. S. Robinson, 1984. Atmospheric correction of LANDSAT MSS Data for a multidate suspended sediment algorithm. *Int. J. Remote Sensing*, Vol. 5, No. 3, pp. 561–576.

Markham, B. L., and J. L. Barker, 1982. *Spectral characterization of the Landsat-D multispectral scanner subsystems.* NASA, GSFC Greenbelt Techn. Memo 83955.

Munday, J. C., 1983. Chromaticity of path radiance and atmospheric correction of Landsat data. *Rem. Sens. of Env.* 25, pp. 525–538.

Munday, J. C., and T. Alföldi, 1975. Chromaticity changes from isoluminous techniques used to enhance multispectral remote sensing data. *Remote Sensing of Environment* 4, pp. 221–236.

———, 1979. Landsat test of diffuse reflectance models for aquatic suspended solids measurement. *Rem. Sens. of Env.* 8, pp. 160–183.

Munday, J. C., T. Alföldi, and C. L. Amos, 1980. Application of a system for automated multidate Landsat measurement of suspended sediment. *Water Quality Bull.*, Vol. 5, No. 1.

Strickland, J. D. H., and T. R. Parsons, 1972. *A practical handbook of sea water analysis.* Bull. Fish. Res. Bd Canada 122.

Sörensen, R. M. (ed.), 1979. *Atmospheric correction of satellite observation of sea water colour.* Recommendations of the Int. Workshop. Commission of the European Communities. Ispra, Italy.

Verdin, J., 1983. *Corrected vs. uncorrected Landsat-4 MSS data.* Landsat Data Users Notes, June 1983.

(Received 19 March 1985; revised and accepted 10 March 1986)

Forthcoming Articles

F. J. Ahern, W. J. Bennett, and *E. G. Kettela,* An Initial Evaluation of Two Digital Airborne Imagers for Surveying Spruce Budworm Defoliation.

Pat S. Chavez, Jr., Digital Merging of Landsat TM and Digitized NHAP Data for 1:24,000-Scale Image Mapping.

William G. Cibula and *Maurice O. Nyquist,* Use of Topographic and Climatological Models in a Geographical Data Base to Improve Landsat MSS Classification for Olympic National Park.

Philip A. Davis, Graydon L. Berlin, and *Pat S. Chavez, Jr.,* Discrimination of Altered Basaltic Rocks in the Southwestern United States by Analysis of Landsat Thematic Mapper Data.

Stephen D. DeGloria and *Andrew S. Benson,* Interpretability of Advanced SPOT Film Products for Forest and Agricultural Survey.

M. S. Elghazali, Mapping from Transmission Electron Micrographs Using the Photogrammetric Plotting System.

S. F. El-Hakim, Real-Time Image Metrology with CCD Cameras.

J. H. Everitt, D. E. Escobar, C. H. Blazquez, M. A. Hussey, and *P. R. Nixon,* Evaluation of the Mid-Infrared (1.45 to 2.0 m) with a Black-and-White Infrared Video Camera.

J. H. Everitt, A. J. Richardson, and *P. R. Nixon,* Canopy Reflectance Characteristics of Succulent and Non-succulent Rangeland Plant Species.

Steven E. Franklin, Terrain Analysis from Digital Patterns in Geomorphometry and Landsat MSS Spectral Response.

Clive S. Fraser, Microwave Antenna Measurement.

D. M. Gerten and *M. V. Wiese,* Microcomputer-Assisted Video Image Analysis of Lodging in Winter Wheat.

Daniel K. Gordon, Warren R. Philipson, and *William D. Philpot,* Fruit Tree Inventory with Landsat Thematic Mapper Data.

A. G. Kerber and *J. B. Schutt,* Utility of AVHRR Channels 3 and 4 in Land-Cover Mapping.

C. P. Lo, Accuracy of Population Estimation from Medium-Scale Aerial Photography.

Daniel S. Long, John E. Taylor, and *Jack McCarthy,* Cessna Aircraft Cabin Door Mount for Photographic and Videographic Cameras.

R. D. Martin, Jr., and *J. L. Heilman,* Spectral Reflectance Patterns of Flooded Rice.

Yukio Mukai, Toshiro Sugimura, Hiroshi Watababe, and *Kuniyasu Wakamori,* Extraction of Areas Infested by Pine Bark Beetle Using Landsat MSS Data.

H. Brad Musick and *Ramona E. Pelletier,* Response of Some Thematic Mapper Band Ratios to Variation in Soil Water Content.

William J. Ripple, Spectral Reflectance Relationships to Leaf Water Stress.

Humberto Rosas, Vertical Exaggeration in Stereo-Vision: Theories and Facts.

Tony Schenk, A Robust Solution to the Line-Matching Problem in Photogrammetry and Cartography.

Hartmut Ziemann and *Sabry F. El-Hakim,* System Calibration and Self Calibration. Part 1: Rotationally Symmetrical Lens Distortion and Image Deformation.